

# A 14-Bit Oversampled SAR ADC With Mismatch Error Shaping and Analog Range Compensation

**Citation for published version (APA):**

Shen, Y., Li, H., Bindra, H. S., Cantatore, E., & Harpe, P. (2023). A 14-Bit Oversampled SAR ADC With Mismatch Error Shaping and Analog Range Compensation. *IEEE Transactions on Circuits and Systems II: Express Briefs*, 70(5), 1719-1723. Article 10077761. <https://doi.org/10.1109/TCSII.2023.3259821>

**Document license:**  
Unspecified

**DOI:**  
[10.1109/TCSII.2023.3259821](https://doi.org/10.1109/TCSII.2023.3259821)

**Document status and date:**  
Published: 01/05/2023

**Document Version:**  
Accepted manuscript including changes made at the peer-review stage

**Please check the document version of this publication:**

- A submitted manuscript is the version of the article upon submission and before peer-review. There can be important differences between the submitted version and the official published version of record. People interested in the research are advised to contact the author for the final version of the publication, or visit the DOI to the publisher's website.
- The final author version and the galley proof are versions of the publication after peer review.
- The final published version features the final layout of the paper including the volume, issue and page numbers.

[Link to publication](#)

**General rights**

Copyright and moral rights for the publications made accessible in the public portal are retained by the authors and/or other copyright owners and it is a condition of accessing publications that users recognise and abide by the legal requirements associated with these rights.

- Users may download and print one copy of any publication from the public portal for the purpose of private study or research.
- You may not further distribute the material or use it for any profit-making activity or commercial gain
- You may freely distribute the URL identifying the publication in the public portal.

If the publication is distributed under the terms of Article 25fa of the Dutch Copyright Act, indicated by the "Taverne" license above, please follow below link for the End User Agreement:

[www.tue.nl/taverne](http://www.tue.nl/taverne)

**Take down policy**

If you believe that this document breaches copyright please contact us at:

[openaccess@tue.nl](mailto:openaccess@tue.nl)

providing details and we will investigate your claim.

# A 14-bit Oversampled SAR ADC With Mismatch Error Shaping and Analog Range Compensation

Yuting Shen, *Graduate Student Member, IEEE*, Hanyue Li, *Graduate Student Member, IEEE*, Harijot Singh Bindra, *Member, IEEE*, Eugenio Cantatore, *Fellow, IEEE*, and Pieter Harpe, *Senior Member, IEEE*

**Abstract**—DAC mismatch is a major challenge for high-resolution ADCs. This paper proposes an analog-detection-based input range compensation technique for high-resolution ADCs with mismatch error shaping (MES). By applying a pre-comparison and suitably switching the DAC MSB, the input loss caused by MES is compensated. By adopting a flying-capacitor sampling technique, the prediction errors found in prior solutions are avoided. The prototype 14-bit SAR ADC achieves 80.4 dB SNDR and 93 dB SFDR in a 4 kHz signal bandwidth with an OSR of 16. It only occupies 0.0034 mm<sup>2</sup> and consumes 0.656  $\mu$ W under a 0.8 V supply, leading to a Schreier figure-of-merit of 178.3 dB. These features make it suitable for miniaturized high-performance IoT and biomedical systems.

**Index Terms**—Analog-to-digital converter (ADC), flying capacitor sampling, input range compensation, mismatch error shaping (MES), successive approximation register (SAR).

## I. INTRODUCTION

THANKS to recent developments, high-resolution SAR ADCs are becoming more and more popular in IoT and bio-recording applications. For example, a 13-bit SAR ADC is used in [1] to read out fetal electrocardiogram signals. If better tolerance against motion artifacts is required, ADCs with even higher resolution are desired. In the above applications, power and area are two critical design concerns. A major challenge for high-resolution SAR ADCs is DAC mismatch, which imposes a minimum used capacitor value and thus has a negative impact on the required power consumption and area.

Many techniques have been proposed to address the DAC mismatch issue [2]–[8]. Among these techniques, mismatch error shaping (MES) is an efficient choice for high-resolution SAR ADCs thanks to its capability of being applied to binary-scaled cells [4]. One disadvantage of MES is that the ADC will lose half of the input range, which tightens the absolute noise requirements for high-resolution systems. To solve this problem, existing solutions can be divided into two categories. The first option is only applying MES to the least significant bits (LSBs) [4], [5]. For segmentation-based methods, part of the input range is still lost and data weighted averaging (DWA) is required to solve the most significant bit (MSB) capacitor mismatch. The second option is to compensate the input range by prediction [6]–[8]. The main challenge for prediction-based

Yuting Shen, Hanyue Li, Haoming Xin, Eugenio Cantatore and Pieter Harpe are with the Department of Electrical Engineering, Eindhoven university of Technology, Eindhoven, The Netherlands. Harijot Singh Bindra is with the Integrated Circuit Design Group, Faculty of Electrical Engineering, Mathematics and Computer Science, University of Twente, Enschede, The Netherlands (e-mail: y.shen@tue.nl).

Manuscript received xx xx, 2023; revised xx xx, 2023.

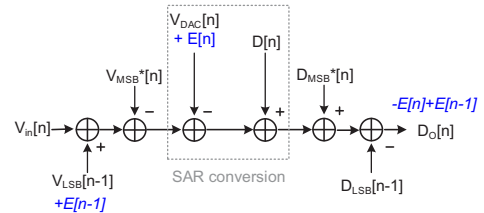


Fig. 1. Principle of MES with input range compensation.

methods is that the prediction might be wrong. Its accuracy is highly related to the oversampling ratio (OSR) of the system (usually requires  $\geq 16$ ) and the existence of interferers.

In this work, an input range compensation technique based on analog detection is proposed. By performing a pre-comparison and switching the DAC MSB accordingly, the input range is then recovered and no DWA is required while MES can be applied to all bits in the converter. By using a flying capacitor sampling technique, the pre-comparison is done after the sampling moment. Hence, prediction errors are avoided. A prototype SAR ADC with a 14-bit resolution is implemented in 65 nm CMOS. As a result, it achieves 80.4 dB SNDR with 0.656  $\mu$ W in a 0.034 mm<sup>2</sup> area.

This paper is organized as follows: Section II reviews the principle of MES with input range compensation. Section III discusses the proposed analog detection and compensation technique with flying capacitor sampling. Section IV presents the circuit implementation in detail. Section V provides the measured results and Section VI draws the conclusion.

## II. REVIEW OF MES WITH INPUT RANGE COMPENSATION

Fig. 1 shows the principle of MES with input range compensation. Mismatch is a relative error. Taking the DAC MSB (1-bit) as a reference, the mismatch of the LSBs (i.e.: all bits except the 1-bit MSB) can result in conversion errors  $E[n]$  at the  $n^{\text{th}}$  conversion cycle. For ADCs with MES, the previous LSB code ( $D_{LSB}[n-1]$ ), together with its conversion error  $E[n-1]$ , will be fed back to the current input signal ( $V_{in}[n]$ ) before SAR conversion. Afterwards,  $D_{LSB}[n-1]$  will be subtracted in the digital domain. During the  $n^{\text{th}}$  SAR conversion, a new  $E[n]$  is generated. This results in a function of  $-E[n] + E[n-1]$  at the output, which behaves as a high-pass filter for DAC mismatch errors. Thus the DAC mismatch errors are 1<sup>st</sup>-order shaped to high frequencies and can be filtered out in an oversampled system.

However, the LSB feedback results in a loss of input signal range. Assume that the original input range of a differential

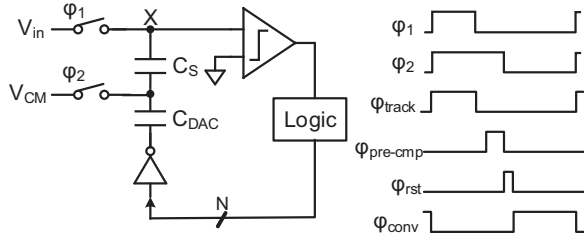


Fig. 2. A simplified diagram of a SAR ADC with the proposed input range compensation technique and its timing diagram.

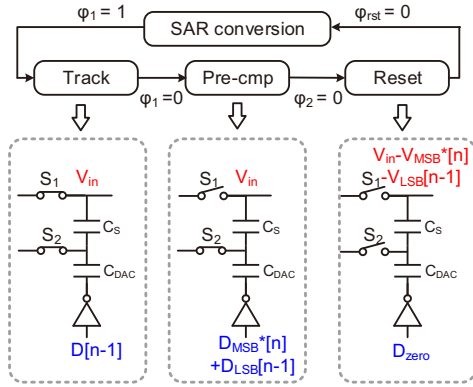


Fig. 3. Circuit operation of the proposed input range compensation technique.

ADC is  $[-V_{ref}, V_{ref}]$ .  $D_{LSB}[n]$  can be any value within  $[-\frac{1}{2}V_{ref}, \frac{1}{2}V_{ref}]$ . Hence, half of the original input range is occupied. The available MSB capacitors, which can generate a  $\pm \frac{1}{2}V_{ref}$  voltage step, can be used to compensate for the input range loss.

A prediction can be done to estimate the direction of overrange. Depending on the predicted signal range, a compensating voltage shift created by the available MSB capacitors can be applied to the input prior to sampling to avoid overrange. Then, this compensation voltage is removed again in the digital domain. In this way, DAC mismatch errors can be shaped without input range loss. Depending on the actual design, either analog or digital, 2-level or 3-level prediction can be adopted [6]–[8].

One drawback of prediction-based methods is that the prediction accuracy is sensitive to OSR and interference. Hence, a certain OSR is required to ensure the prediction accuracy, which is necessary to avoid conversion errors.

### III. PROPOSED INPUT RANGE COMPENSATION WITH ANALOG DETECTION

#### A. Architecture and operation

This work adopts the same principle described in Fig. 1. However, instead of prediction, this work proposes an input range compensation technique based on analog detection. A simplified diagram of a SAR ADC with the proposed input range compensation technique and its timing diagram are shown in Fig. 2. Note that  $C_{DAC}$  represents an N-bit binary-scaled array of capacitors, as required for the SAR operation. Further, a single-ended diagram is shown here for simplicity.

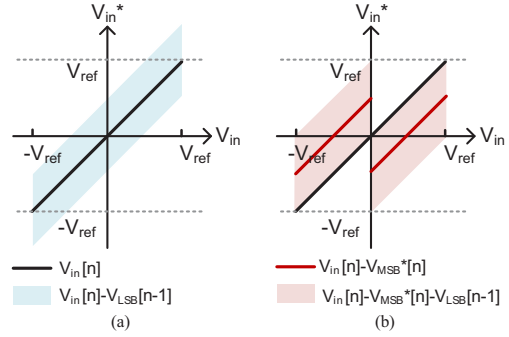


Fig. 4. A conceptual diagram of the equivalent input signal without (a) and with (b) input range compensation.

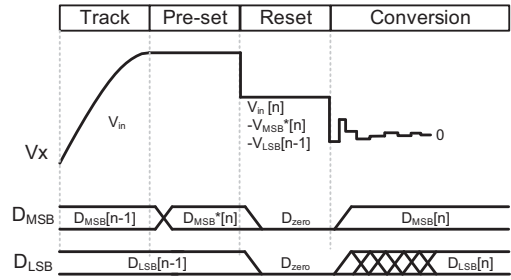


Fig. 5. An example of the time-domain behavior for the signal at the comparator input and the DAC control signals.

Compared to a conventional top-plate sampled SAR ADC, a separate sampling capacitor ( $C_S$ ) in series with the DAC capacitors ( $C_{DAC}$ ) and an extra sampling switch are introduced. The two sampling switches ( $S_1$  and  $S_2$ ) are controlled by  $\varphi_1$  and  $\varphi_2$ , respectively. Besides, an extra pre-comparison phase is generated after the sampling moment and the reset phase is positioned after the pre-comparison phase and before the SAR conversion phase.

As shown in Fig. 3, the circuit-level operation consists of 4 phases, tracking, pre-comparison, reset and SAR conversion. The signal processing for the  $n^{th}$  cycle starts at the rising edge of  $\varphi_1$ . First, during the tracking phase, the sampling capacitor ( $C_S$ ) tracks the input. The DAC capacitors remain at their state of the previous cycle. After  $V_{in}$  is sampled on  $C_S$  at the falling edge of  $\varphi_1$ , a pre-comparison using the existing comparator of the ADC will be done to determine the polarity of  $V_{in}$ . While the sampling capacitor continues holding the input, the DAC MSB capacitors are now set to the polarity of the input signal ( $D_{MSB}^*[n-1]$ ), which was detected by the pre-comparison. For example, if  $V_{in} > 0V$ , the MSB capacitors are set to  $V_{ref}$ . The DAC LSB capacitors still remain at their previous value ( $D_{LSB}[n-1]$ ). Then, at the falling edge of  $\varphi_2$ ,  $S_2$  is opened. The sampling capacitor is now floating. Both MSB and LSB capacitors are reset by changing the control codes from  $D_{MSB}^*[n] + D_{LSB}[n]$  to  $D_{zero}$ . Here,  $D_{zero}$  represents the DAC code in the reset state. The equivalent sampled signal at the comparator input ( $V_{in}^*$ ) becomes  $V_{in}[n] - V_{MSB}^*[n] - V_{LSB}[n-1]$ , where  $V_{LSB}$  enables the MES operation, and  $V_{MSB}^*$  creates the compensation to prevent overrange. As what is conceptually

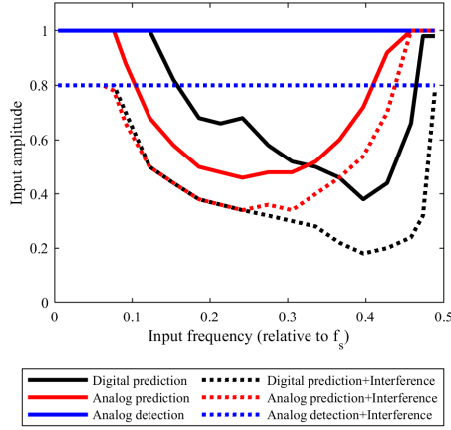


Fig. 6. Simulated input amplitude as a function of input frequency with and without interference.

shown in Fig. 4, the input range of the ADC is recovered to  $[-V_{ref}, V_{ref}]$  when compensation is applied. A regular SAR conversion starts afterwards and sets the DAC control code to  $D[n]$ , which represents the DAC value at the  $n^{th}$  cycle. An example of the time-domain behavior for the signal at the comparator input ( $V_x$ ) and the DAC control signals are shown in Fig. 5.

The main advantage of this detection scheme is that it determines the compensation voltage after sampling, whereas previous prediction methods determine the compensation prior to the sampling moment. As a result, the proposed method does not suffer from prediction errors.

### B. Discussions

By using the proposed analog-detection-based input range compensation, two samplings steps are performed and now the sampling noise power is equal to:

$$\frac{2kT}{C_S} + \frac{2kT}{C_{DAC}} \quad (1)$$

To minimize the noise overhead,  $C_S$  could be set to for instance  $2.7 C_{DAC}$ , which degrades the SNR by only 1.4 dB.

On the other hand, by performing two samplings steps, the information of the current input signal can be known without prediction, and thus without errors. For comparison against prior prediction schemes, Fig. 6 shows the maximum input amplitude without overrange as a function of the input frequency with and without an interference tone, simulated using a behavioral model. If interference is enabled, it is set to a 20% full-scale tone at  $0.4f_s$ , so it can be compared against the results in [6], [8]. Thus, ideally, the input signal should reach 100% full-scale without interference or 80% full-scale with interference, unless prediction errors occur. As can be seen, with digital [6] or analog [8] prediction schemes, the maximum input amplitude drops for higher input frequencies due to prediction errors, which thus implies a minimum required OSR to limit the signal bandwidth. Besides, the existence of interference will further degrade the prediction

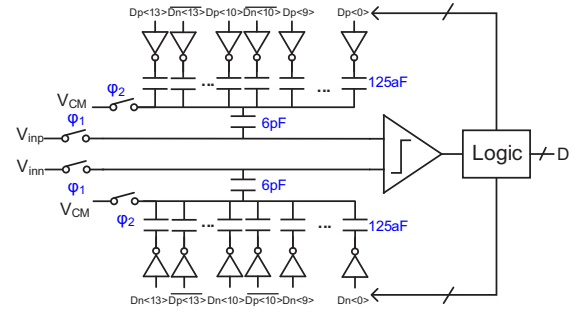


Fig. 7. Proposed SAR ADC with MES and analog range compensation.

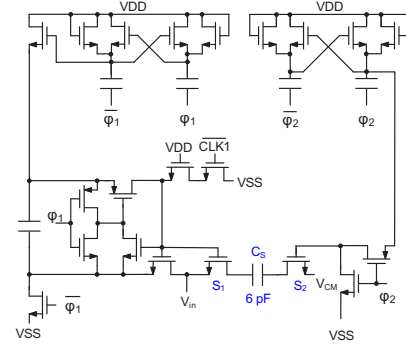


Fig. 8. Schematic of the proposed flying capacitor sampling circuit.

accuracy and thus an even higher OSR is required. The proposed analog detection method can avoid these concerns and the performance remains constant regardless of OSR.

## IV. CIRCUIT IMPLEMENTATION

Fig. 7 shows the schematic of this work, which consists of a track and hold circuit, a 14-bit capacitive DAC, a dynamic biased comparator and asynchronous logic.

### A. Track and hold

The schematic design of the new track and hold circuit is shown in Fig. 8, which consists of sampling switches  $S_1$ ,  $S_2$  and a sampling capacitor  $C_S$ .  $S_2$  is driven by a boosted clock for simplicity and lower power overhead.  $S_1$  is driven by a bootstrapping circuit for higher linearity requirements.

Theoretically, the absolute value of  $C_S$  does not affect the operation of the ADC. In the actual implementation, the mismatch of  $C_S$  and the mismatch of parasitic capacitances may result in even order distortion and affect the SNDR for a high-linearity system. A large  $C_S$  results in lower sampling noise and better matching. However, it may also degrade the maximum operation speed of the ADC and costs more area. Fortunately, since  $C_S$  is only one capacitor, its implementation is relatively area-efficient compared to DAC capacitors. As a trade-off, in this work,  $C_S$  is implemented by regular metal-oxide-metal capacitors with a minimal spacing of 100nm and its value is chosen to be 6 pF. It occupies 15% of the ADC area and results in 93 dB SNR with 2.2 pF DAC capacitance for an input range of 1.6 V and an oversampling ratio of 16. A 7% mismatch of  $C_S$  versus  $C_{DAC}$  can be tolerated to achieve above 100 dB SFDR, which is easy to satisfy with a 6 pF capacitance in the used technology.

TABLE I  
 PERFORMANCE SUMMARY AND COMPARISON

	[2]	[3]	[4]	[5]	[6]	[7]	[8]	This work
DAC mismatch calibration	Vector-based DEM	Dither	MES +DWA	MES +DWA	MES +Digital prediction	MES +Digital prediction	MES +Analog prediction	MES +Analog detection
Technology [nm]	40	65	55	40	40	65	65	65
Supply voltage [V]	1.1	0.8	1.2	1.1	1.1	1.2	0.8	0.8
Sample rate [kS/s]	32000	128	1000	12800	2000	1000	128	128
Oversampling ratio	64	16	250	64	25	16	16	16
Bandwidth [kHz]	250	4	4	100	40	31.25	4	4
Power [ $\mu$ W]	4700	1.37	15.7	1998	67.4	7.3	0.98	0.656
SNDR [dB]	94.8	79.1	96.1	98.3	90.5	80	84.5	80.4
SFDR [dB]	103.0	87.1	105.1	108.5	102.2	98	103	93
DR [dB]	96	-	-	101.2	94.3	81.4	85	80.5
FoM <sub>W</sub> [fI/conv-step] <sup>1</sup>	209.3	23.2	37.61	148.6	30.77	14.3	9.4	9.57
FoM <sub>S</sub> [dB] <sup>2</sup>	172.1	173.8	180	175.3	178.2	176.3	180.6	178.3
Area [mm <sup>2</sup> ]	0.37	0.18	0.072	0.48	0.061	0.043	0.033	0.034

<sup>1</sup>  $FoM_W = Power / (2^{ENOB} \times 2 \times BW)$

<sup>2</sup>  $FoM_S = SNDR + 10 \times \log_{10}(BW/Power)$

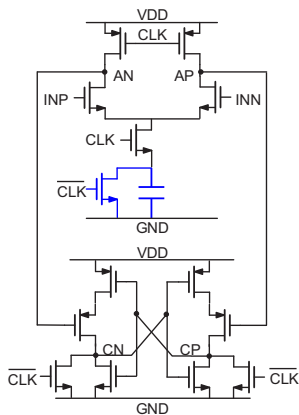


Fig. 9. Schematic of the comparator [9].

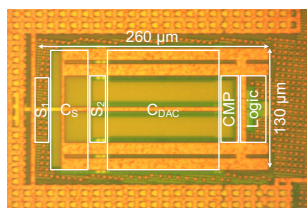


Fig. 10. Chip micrograph.

### B. Comparator

The comparator is another bottleneck for high-resolution SAR ADCs and one of the dominant power consumption sources. Similar to a regular SAR ADC, comparator offset in this work occupies a small part of the ADC input range, but it does not affect the linearity of the ADC. Fig. 9 shows the schematic design of the used dynamic comparator, which consists of a dynamic bias pre-amplifier and a latch. A tail capacitor and a NMOS switch are added to the bottom of the pre-amplifier to reduce the energy consumption by means of self quenching and to pre-dominantly operate in weak inversion for maximizing its  $gm/Id$  [9]. In this work, a 300 fF tail capacitor is used, which reduces the comparator power by about 23%.

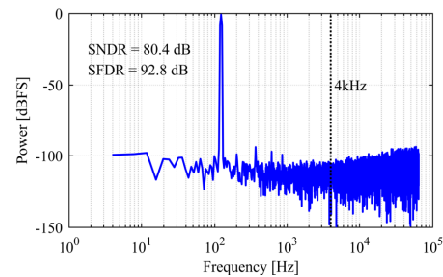
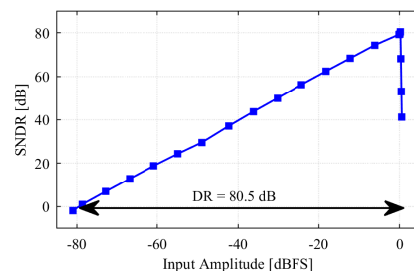

 Fig. 11. Measured spectrum for  $f_{in} = 122$  Hz, at 128 kS/s and an OSR of 16.


Fig. 12. Measured SNDR versus input amplitude.

## V. MEASUREMENT RESULTS

The prototype ADC is implemented in 65 nm CMOS as shown in Fig. 10. It occupies an active area of 0.034 mm<sup>2</sup> and was measured to consume 0.656  $\mu$ W at a sampling rate of 128 kHz from a 0.8 V supply.

The measured spectrum with a 128 kHz sampling rate and a 122 Hz input frequency is shown in Fig. 11. The peak-to-peak input signal range is around 1.36 V. With an OSR of 16, the prototype ADC achieves 80.4 dB SNDR and 92.8 dB SFDR in a 4 kHz signal bandwidth. The DAC mismatch error is first order shaped. Fig. 12 shows the measured SNDR versus input amplitude. The measured dynamic range (DR) of this prototype is 80.5 dB.

Fig. 13 shows the measured SNDR versus input frequency for a full range input and an OSR of 1. Due to the lack of oversampling, the SNDR in this case is lower than before since all noise and distortion contributions count. However, this result confirms that the ADC does not saturate for any



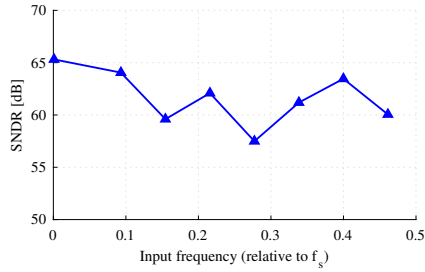


Fig. 13. Measured SNDR versus input frequency for a full range input (OSR = 1).

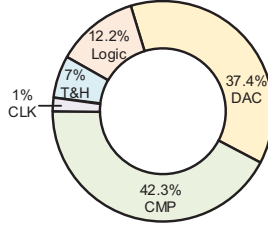


Fig. 14. Power breakdown of the ADC.

input frequency, as this would otherwise lead to a major SNDR reduction. For prior-art prediction methods, their SNDR will quickly drop for high input frequencies due to prediction errors.

Fig. 14 shows the post-layout simulated power breakdown of the ADC. Thanks to MES, small DAC capacitors can be used and the DAC switching requires only 37.4% of the total power.

Table I summarizes the performance of this work and compares it to state-of-the-art designs with on-chip DAC mismatch calibration techniques. Compared to [2-8], this work achieves competitive energy and area efficiency with a simple architecture and zero prediction errors.

## VI. CONCLUSION

This article presents a 14-bit SAR ADC with mismatch error shaping and analog-detection-based input range compensation. The proposed pre-comparison technique with flying capacitor sampling, can detect the input range without prediction errors. Combined with MES and suitable MSB switching, the DAC mismatch error can be shaped without input range loss. The prototype ADC fabricated in 65 nm CMOS occupies an area of 0.034 mm<sup>2</sup> and consumes 0.656  $\mu$ W at a sampling frequency of 128 kHz. The achieved SNDR and SFDR are 80.4 dB and 92.8 dB, respectively. The resulting Schreier FoM is 178.3 dB and the resulting Walden FoM is 9.57 fJ/conversion.

## ACKNOWLEDGMENT

This work is financially supported by the Dutch Research Council (NWO) under Grant 16594 and we would kindly acknowledge EUROPRACTICE for its MPW and design tool support.

## REFERENCES

- [1] R. van Wegberg, W. Sijbers, S. Song, A. Breeschoten, P. Vis, M. Konijnburg, H. Jiang, M. Rooijackers, T. Berset, J. Penders, C. Van Hoof, and N. Van Helleputte, "A 5-Channel Unipolar Fetal-ECG Readout IC for Patch-Based Fetal Monitoring," *IEEE Solid-State Circuits Letters*, vol. 2, no. 9, pp. 71–74, 2019.
- [2] W. Shi, X. Wang, X. Tang, A. Mukherjee, R. Theertham, S. Pavan, L. Jie, and N. Sun, "A 0.37mm<sup>2</sup> 250kHz-BW 95dB-SNDR CTDSM with Low-Cost 2nd-order Vector-Quantizer DEM," in *2022 IEEE Custom Integrated Circuits Conference (CICC)*, 2022, pp. 1–2.
- [3] P. Harpe, E. Cantatore, and A. van Roermund, "An oversampled 12/14b SAR ADC with noise reduction and linearity enhancements achieving up to 79.1dB SNDR," in *2014 IEEE International Solid-State Circuits Conference Digest of Technical Papers (ISSCC)*, 2014, pp. 194–195.
- [4] Y.-S. Shu, L.-T. Kuo, and T.-Y. Lo, "An oversampling SAR ADC with DAC mismatch error shaping achieving 105dB SFDR and 101dB SNDR over 1kHz BW in 55nm CMOS," in *2016 IEEE International Solid-State Circuits Conference (ISSCC)*, 2016, pp. 458–459.
- [5] K. Hasebe, S. Etou, D. Miyazaki, T. Iguchi, Y. Yagishita, M. Takasaki, T. Nogamida, H. Watanabe, T. Matsumoto, and Y. Katayama, "A 100kHz-Bandwidth 98.3dB-SNDR Noise-Shaping SAR ADC with Improved Mismatch Error Shaping and Speed-Up Techniques," in *2022 IEEE Symposium on VLSI Technology and Circuits (VLSI Technology and Circuits)*, 2022, pp. 56–57.
- [6] J. Liu, X. Wang, Z. Gao, M. Zhan, X. Tang, and N. Sun, "A 40kHz-BW 90dB-SNDR Noise-Shaping SAR with 4 $\times$  Passive Gain and 2nd-Order Mismatch Error Shaping," in *2020 IEEE International Solid-State Circuits Conference - (ISSCC)*, 2020, pp. 158–160.
- [7] H. Li, Y. Shen, H. Xin, E. Cantatore, and P. Harpe, "A 7.3- $\mu$ W 13-ENOB 98-dB SFDR Noise-Shaping SAR ADC With Duty-Cycled Amplifier and Mismatch Error Shaping," *IEEE Journal of Solid-State Circuits*, vol. 57, no. 7, pp. 2078–2089, 2022.
- [8] Y. Shen, H. Li, H. Xin, E. Cantatore, and P. Harpe, "A 103-dB SFDR Calibration-Free Oversampled SAR ADC With Mismatch Error Shaping and Pre-Comparison Techniques," *IEEE Journal of Solid-State Circuits*, vol. 57, no. 3, pp. 734–744, 2022.
- [9] H. S. Bindra, C. E. Lokin, D. Schinkel, A.-J. Annema, and B. Nauta, "A 1.2-V Dynamic Bias Latch-Type Comparator in 65-nm CMOS With 0.4-mV Input Noise," *IEEE Journal of Solid-State Circuits*, vol. 53, no. 7, pp. 1902–1912, 2018.